Biochimica et Biophysica Acta 1840 (2014) 1014–1027

Contents lists available at ScienceDirect

Biochimica et Biophysica Acta

journal homepage: www.elsevier.com/locate/bbagen

DNA damage dependent activation of checkpoint kinase-1 and mitogen-activated protein kinase-p38 are required in malabaricone C-induced mitochondrial cell death

Mrityunjay Tyagi [1], Rahul Bhattacharyya, Ajay Kumar Bauri, Birija Sankar Patro [1], Subrata Chattopadhyay *

Bio-Organic Division, Bhabha Atomic Research Centre, Mumbai 400085, India

ARTICLE INFO

Article history:
Received 7 May 2013
Received in revised form 19 November 2013
Accepted 20 November 2013
Available online 27 November 2013

Keywords:
ATM/ATR
DNA strand break
Lung cancer cell
Malabaricone C
MAPK
Mitochondrial dysfunction

ABSTRACT

Background: Given that lung cancer is the second leading cause of cancer-related deaths with low survival rates, the project was aimed to formulate an efficient drug with minimum side effects, and rationalize its action mechanistically.
Methods: Mitochondria deficient cells, shRNA-mediated BCL2 and ATM depleted cells and pharmacological inhibition of DNA-damage response proteins were employed to explore the signaling mechanism governed between nucleus and mitochondria in response to mal C.
Results: Mal C decreased cell viability in three lung carcinoma cells, associated with DNA damage, p38-MAPK activation, imbalance in BAX/BCL2 expression, mitochondrial dysfunction and cytochrome-c release. Mitochondria depletion and p38-MAPK inhibition made A549 cells extremely resistant, but BCL2 knock-down partially sensitized the cells to mal C treatment. The mal C-induced apoptosis in A549 cells was initiated by DNA single strand breaks that led to double strand breaks (DSBs). DSB generation paralleled the induction of ATM- and ATR-mediated CHK1 phosphorylation. ATM silencing and ATR inhibition partially attenuated the mal C-induced p38-MAPK activation, CHK1 phosphorylation and apoptosis, which were completely suppressed by CHK1 inhibition.
Conclusions: Mal C activates the ATM-CHK1-p38 MAPK cascade to cause mitochondrial cell death in lung carcinoma cells.
General significance: Given that mal C has appreciable natural abundance and is non-toxic to mice, further in vivo evaluation would help in establishing its anti-cancer property.

1. Introduction

Lung cancer is the second leading cause of cancer-related deaths all over the world, with low survival rates in advanced stages [1]. The poor prognosis is largely attributable to the inherent or acquired resistance in cancer cells against conventional chemotherapy. Dysregulation in apoptotic pathways is one of the major causes of drug resistance, although other mechanisms including improved DNA repair, drug transport and detoxification also play significant roles [2]. There is a burgeoning interest in small organic molecules, capable of switching their redox status, as these can often cleave DNA and/or target mitochondria, and hence can be used as anti-cancer agents. The molecules, which permeabilize mitochondria in cancer cells can also sensitize cancer cells further to genotoxic drugs [2]. These molecules modulate the inhibition of the BCL-2 anti-apoptotic family proteins and activation of BAX/BID pro-apoptotic mimetics by reactive oxygen species (ROS)-dependent or independent processes to induce mitochondrial permeability transition (MPT) pore opening [2,3]. This causes cytochrome c release, formation of apoptosome assembly, and activation of the executioner caspases [4]. Of late, the mitogen-activated protein kinase (MAPK) pathways have emerged as crucial signaling events that regulate mitochondrial dysfunction in response to various chemotherapeutic drugs, stress signals, ionizing radiation, UV and tumor necrosis factor-α. Amongst the MAPKs, c-Jun N-terminal kinase (JNK) and p38 are weakly activated by growth stimuli, but respond strongly to chemotherapeutic drugs [5–8]. Activation of these kinases is associated with ameliorating apoptosis in cancer cells. Moreover, JNK and/or p38 MAPKs-mediated cell death is often accompanied by regulating the redistribution of BAX from the cytoplasm to the mitochondria [9] and modulating BCL-2 phosphorylation status in response to various stimuli, suggesting an upstream role of MAPK to mitochondrial dysfunction [8,10]. Many chemotherapeutic agents, like Taxol® (paclitaxel), cisplastin, vinblastine etc. are known to sensitize cancer cells through the activation of p38 and/or JNK pathways [11,12].

Because of their known low/non toxicity towards normal cells, exploration of dietary small molecules as chemo-preventive agents is one of the major goals in recent anti-cancer research. The fruit rind of the plant, *Myristica malabarica* (*Myristicaceae*) (popularly known as

* Corresponding author. Tel.: +91 22 25592399; fax: +91 22 25505151.
E-mail address: schatt@barc.gov.in (S. Chattopadhyay).
[1] Equal contributions.

0304-4165/$ – see front matter © 2013 Elsevier B.V. All rights reserved.
http://dx.doi.org/10.1016/j.bbagen.2013.11.020

rampatri, Bombay mace or false nutmeg) is used as an exotic spice in various Indian cuisines. This is credited with hepatoprotective, anticarcinogenic and antithrombotic properties, and also used as a constituent in some Ayurvedic preparations such as pasupasi and Muthu-Marunthu [13]. Several herbal formulations containing *M. malabarica* are also claimed to possess antitumor effect [13,14]. Earlier, we have found

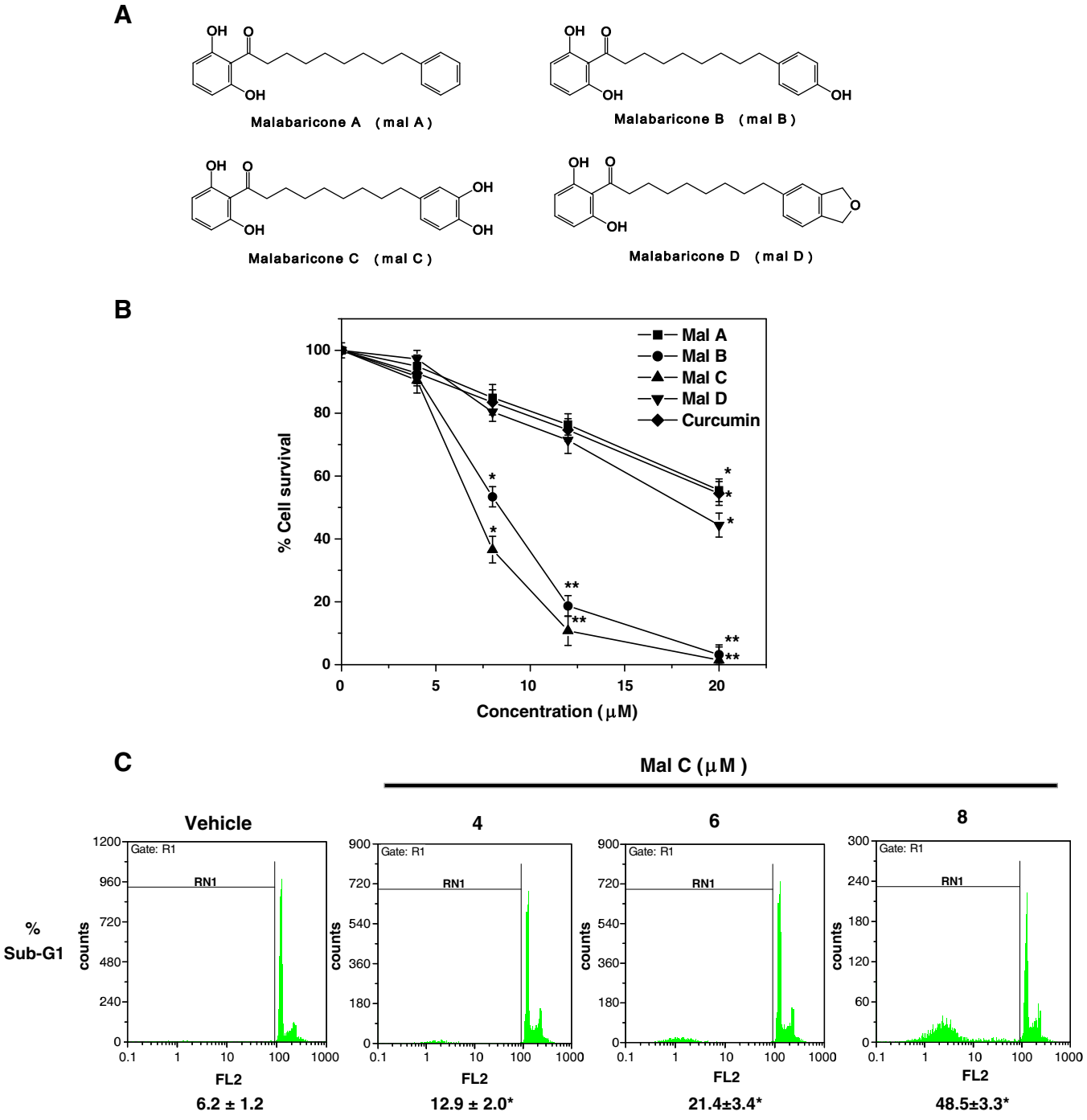

Fig. 1. Mal C induces apoptosis in A549 lung carcinoma cells. (A) Chemical structures of the malabaricones. (B) Cytotoxicity of the malabaricones and curcumin. A549 cells (6000 cells/well), grown in 96-well plates were treated with vehicle (0.1% DMSO) or increasing concentrations of the malabaricones and curcumin. The cell viability was assessed by the MTT assay after 48 h. The results are expressed in percentage survival considering that of the vehicle-treated control cells as 100. The experiments were repeated three times with similar results. All determinations were made in four replicates, and the values are means ± S. E. M. $^{*}P < 0.01$, $^{**}P < 0.001$ compared to vehicle control. (C) Flow cytometric analysis of sub-G1 (apoptotic) population in response to mal C treatment. A549 cells were treated with mal C (4, 6 and 8 μM) for 24 h. Twenty thousand cells in each treatment were acquired using a flow cytometer. The Sub-G1 region (RN1) represents the percentage of cells undergoing apoptosis. The abbreviation FL2 in the histogram represents intensity of the red fluorescence of propidium dye, acquired in channel-2. The experiments were repeated four times with similar results. All determinations were made in three replicates, and the values are means ± S. E. M. $^{*}P < 0.01$ compared to vehicle control. (D) Activities of caspases-9, -3 and -8. The A549 cells (1×10^6 cells/well) were incubated with vehicle or mal C (6 μM) for 24 h, and the activities of the caspases estimated. Similar analyses were also carried out using cell extracts incubated with specific caspases inhibitors (each 20 μM) for 15 min. The experiments were repeated three times with similar results, all determinations were made in four replicates, and the values are means ± S. E. M. $^{*}P < 0.05$, $^{**}P < 0.01$ compared to vehicle control, $^{\#\#}P < 0.01$ compared to mal C-treatment. (E) Expressions of caspases. The A549 cells were incubated with vehicle or mal C (6 μM) for different time periods, and the activation of the caspases was assessed by the appearance of respective cleaved caspases in the whole cell extracts by immunoblots. The experiments were repeated three times with similar results, and the values are means ± S. E. M. $^{*}P < 0.05$ compared to vehicle control. ^— represents non-specific protein bands in procaspase-3 blot. $^{\$}$ — represents two cleaved caspase-9 bands, 37 and 35 KD respectively.

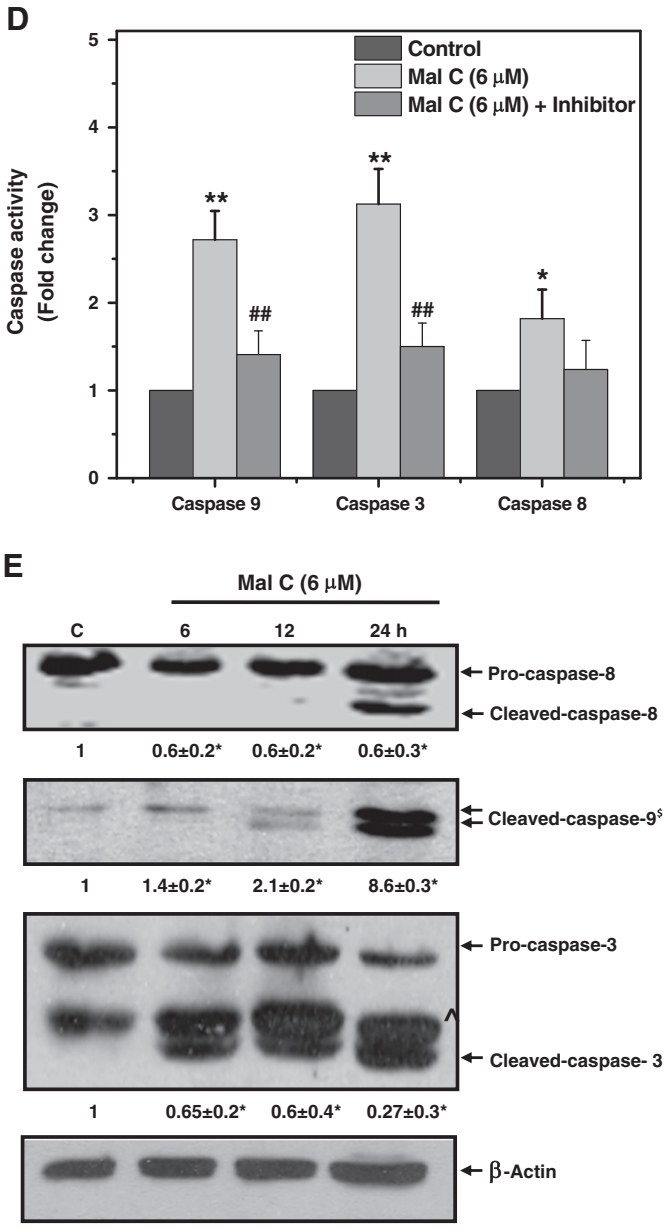

Fig. 1 (*continued*).

that amongst the four malabaricones A–D (designated as mal A–D), isolated from its extract, mal B and mal C possess superior antioxidant, anti-inflammatory, and anti-ulcer properties [15–17]. The chemical structures of mal AD are shown in Fig. 1A. Mal C, containing a B-ring catechol moiety showed significantly better Cu(II)-dependent nuclease activity than its partially methylated congener, mal B as well as curcumin, explaining its better toxicity than curcumin against the MCF-7 human breast cancer cell line [18].

In view of this, presently we studied the effect of mal C on the proliferation of the human non-small cell lung cancer (A549, NCI-H23, and NCI-H460) cell lines. In particular, the possible involvement of nuclear DNA and mitochondrial damages in the mal C-mediated apoptosis in highly invasive and metastatic A549 cells was addressed. We also established the cross-talks between the signaling pathways and apoptotic cell death machinery in the process. For comparison, the antiproliferative property of the other malabaricones (mal A, B and D) against the A549 cell line was also assessed. Our results clearly revealed that the mal C-induced DNA double strand breaks (DSBs) activates ataxia telangiectasia mutated (ATM)/ataxia telangiectasia and Rad related (ATR)-checkpoint kinase-1 (CHK1) and p38 MAP kinases, which in turn, severely perturbs mitochondrial function to release apoptotic factors.

2. Materials and methods

2.1. Chemicals

Mal A–D were isolated, purified and characterized as reported previously [15,19]. VP-16, 3-(4,5-dimethylthiazol-2-yl)-2,5-diphenyltetrazolium bromide (MTT), N-acetylcysteine (NAC), uridine, ethidium bromide (EtBr), sodium pyruvate, UCN-01, annexin-V kit, antibodies for cytochrome c and caspases-3, -8, -9, as well as kits of caspases-3, -8, -9 activities were procured from Sigma Chemicals (St. Louis, MO). Other chemicals used were: Dulbecco's modified Eagle's medium (DMEM, HiMedia, Mumbai), fetal bovine serum (FBS, Gibco Life Technologies, Carlsbad, CA), and U0126, SB203580, SP600125 and KU55933 (Calbiochem, Gibbstown, NJ). Lipofectamine reagent was from Invitrogen (Carlsbad, CA), while antibodies for BAX, BCL-2, and

β-actin were from Cell Signaling Technology Inc. (Danvers, MA). Lumi-Light PLUS western blotting kit and cell death detection PLUS kit were procured from Roche Applied Science (Baden-Wurttemberg, Mannheim). Schisandrin B was purchased from LKT laboratories (St. Paul, MN, USA).

2.2. Cell culture

The A549, NCI-H460 and NCI-H23 cell lines were procured from the National Centre for Cell Science, Pune, India. The cells were cultured in DMEM medium, supplemented with 10% FBS, 100 U/ml penicillin and 100 μg/ml streptomycin. The cells were grown at 37 °C under an atmosphere of 5% CO_2.

2.3. MTT assay

The cytotoxic effects of the malabaricones, curcumin and VP-16 were determined by the MTT reduction assay, as reported earlier [18].

2.4. Comet assay and microscopy

Mal C-induced DSBs at different time points was assessed by neutral comet assay [20]. To see the interaction of mal C with nuclear DNA under cellular conditions, cells were pre-incubated with increasing concentrations of mal C for 1 h and subsequently stained with Hoechst 33342 (20 μM, 15 min). Cells were washed, mounted on glass slides with 70% glycerol, and analyzed under Axioskop II Mot plus (Zeiss) microscope (40× optics). Mitochondria were stained with MitoTracker Red (Invitrogen, Carlsbad, CA) and analyzed by fluorescence microscopy [21].

2.5. Determination of apoptosis

Cytoplasmic release of fragmented chromatin and activation of caspases-3, -8 and -9 were assayed as described previously [22]. For the caspase inhibition studies, the mal C-treated cell lysates were incubated with the inhibitory peptides (each 20 μM), Z-LEHD-FMK (caspase-9 specific), Ac-DEVD-CHO (caspase-3 specific) and Ac-IETD-CHO (caspase-8 specific) for 15 min followed by analysis of the activities of the respective enzymes.

2.6. Generation of mitochondria-deficient A549-ρ^o cells

The mitochondria-deficient A549-ρ^o cells were generated and maintained as described previously [23] with minor modifications. Briefly, the A549 cells were maintained in a complete medium supplemented with 1 mM sodium pyruvate, 1 mM uridine and 60 ng/ml EtBr (24 passages for 8 weeks). The A549 cells, cultured in medium without EtBr served as the control (wild-type A549-ρ^+). Mitochondria depletion in the A549-ρ^o cells was confirmed by analyzing the loss of mitochondria specific protein, cytochrome oxidase IV. The A549-ρ^o cells also showed a disrupted mitochondrial architecture, as confirmed from the severely low staining by the mitochondria-specific dye, MitoTracker Red. For treatment, A549-ρ^o and A549-ρ^+ cells were treated with EtBr-free ρ^o medium containing pyruvate and uridine as mentioned above.

2.7. Flow cytometric analysis of annexin V binding, sub-G1 population and mitochondrial transmembrane potential ($\Delta\Psi_m$)

The hypodiploid DNA content (sub-G1), as a marker for apoptosis was analyzed by flow cytometry. Briefly, the cells were collected, washed with cold PBS and incubated in PBS containing Triton X-100 (0.1%), propidium iodide (PI) (40 μg/ml) and RNAse A (100 μg/ml) for 30 min at 37 °C, and the DNA content of the nuclei was registered. The flipping of phosphatidyl serine (PS) was assessed by using annexin V/PI apoptosis detection kit as per the manufacturer's instructions. $\Delta\Psi_m$ was measured using a potential-sensitive dye, JC-1 [21]. The flow cytometry results were analyzed by a PartecCyflow Space cytometer using the Flowjo Software.

2.8. Immunoblots

Cells were treated with mal C as described in the respective figure legends. The cell lysates, prepared from the floating as well as attached cells were used for the western blots as described previously [22]. Protein amounts (arbitrary unit, mean ± SEM) are quantified by density-scanning results of three independent experiments, considering that of untreated control cells as 1.

2.9. Stable transfection of A549 cells

The A549 cells were transfected with plasmids (Imgenex, San Diego, CA) encoding scrambled short-hairpin RNA (shRNA) to generate BCL2-WT cells or shRNA against BCL2 to generate BCL2 knock down cells (BCL2-KD) using lipofectamine 2000. To generate stable ATM knock down cells (ATM-KD), the cells were exposed to lentiviral particles encoding scrambled shRNA (ATM-WT cells) or targeting ATM (Santa Cruz Biotechnology, Santa Cruz, CA) to generate ATM-KD cells using polybrene. The BCL2-KD, ATM-KD and respective WT cells were grown for two weeks in a medium containing G418 (800 μg/ml) or puromycin (1 μg/ml). Several antibiotic-resistant clones were expanded and screened for the BCL-2 and ATM proteins. The clones with the lowest expression were selected for the studies and maintained further in the presence of G418 (300 μg/ml) or puromycin (0.5 μg/ml).

2.10. Statistical analysis

The data were analyzed by paired *t*-test and one-way analysis of variance (ANOVA). Analyses were considered significantly different at $P < 0.01$, $P < 0.05$, and $P < 0.001$. Values are expressed as mean ± standard error of mean (S.E.M).

3. Results

3.1. Mal C induces apoptosis in A549 cells

The malabaricones and the positive control (curcumin) dose-dependently induced cell death in the A549 cells (Fig. 1B), with the IC50 values of 19.2 ± 4.2 μM (mal A), 8.4 ± 2.5 μM (mal B), 7.0 ± 1.8 μM (mal C), 20.3 ± 5.1 μM (mal D) and 41.7 ± 6.2 μM (curcumin) after 48 h of incubation. Interestingly, mal C induced maximum cell death even at 24 h with no further increase with time (Supplementary Fig. SL1). Further, mal C and curcumin also reduced viability of other lung carcinoma cell lines with IC_{50} of 7.7 ± 2.1 μM and 27.3 ± 4.2 μM for NCI-H460, 9.9 ± 2.7 μM and 22.8 ± 4.0 μM for NCI-H23, and 12.4 ± 3.4 μM and 26.2 ± 3.6 μM for NCI-H522 cells (Supplementary Fig. SL2). Based on these results, mal C was chosen for further studies to elucidate its anti-cancer property in A549 lung carcinoma cells. Mal C showed slightly better cytotoxicity to the A549 cells than mal B. However, we preferred mal C over mal B for all subsequent studies due to its significantly higher natural abundance and ease of isolation from the plant extract.

To assess whether the cell death induced by the mal C involves apoptosis, we looked for apoptosis-specific (i) morphological changes, (ii) annexin-V/PI staining, (iii) sub G1 population, and (iv) enrichment of histone-associated oligonucleosome DNA fragments in the cytoplasm in the mal C-treated cells. Phase-contrast microscopy revealed a concentration dependent alteration in cell morphology with increasing number of shrinking cells with blebbed membranes in response to mal C treatment (Supplementary Fig. SL3). The flow cytometry analyses also clearly revealed that mal C concentration-dependently increased annexin-V-positive cells (Supplementary Fig. SL4) and sub-G1 population (Fig. 1C). A similar concentration-dependent enrichment of

cytoplasmic oligonucleosome in the A549 cells was induced by mal C (Supplementary Fig. SL5). The apoptosis induced by mal C at a 6 fold lower concentration (4 μM) was comparable to that by the positive control, etoposide (25 μM) (Supplementary Fig. SL5).

Next, we investigated whether caspase activation is required for the mal C-induced apoptosis. At 24 h, mal C (6 μM) stimulated the activities of caspase-9 (~2.7 fold, $P < 0.001$) and caspase-3 (~3.1 fold, $P < 0.001$) with minimal increase in the caspase-8 activity, compared to the untreated control cells (Fig. 1D). Such activation was abrogated in the presence of the respective specific caspases inhibitors (each 20 μM). Consistent with these, our immunoblots showed increased activation of caspase-3 and caspase-9 (represented by the cleavage of respective pro-forms) at 6 h, while caspase-8 activation was increased after 24 h in response to mal C treatment (Fig. 1E). Moreover, cells pre-incubated

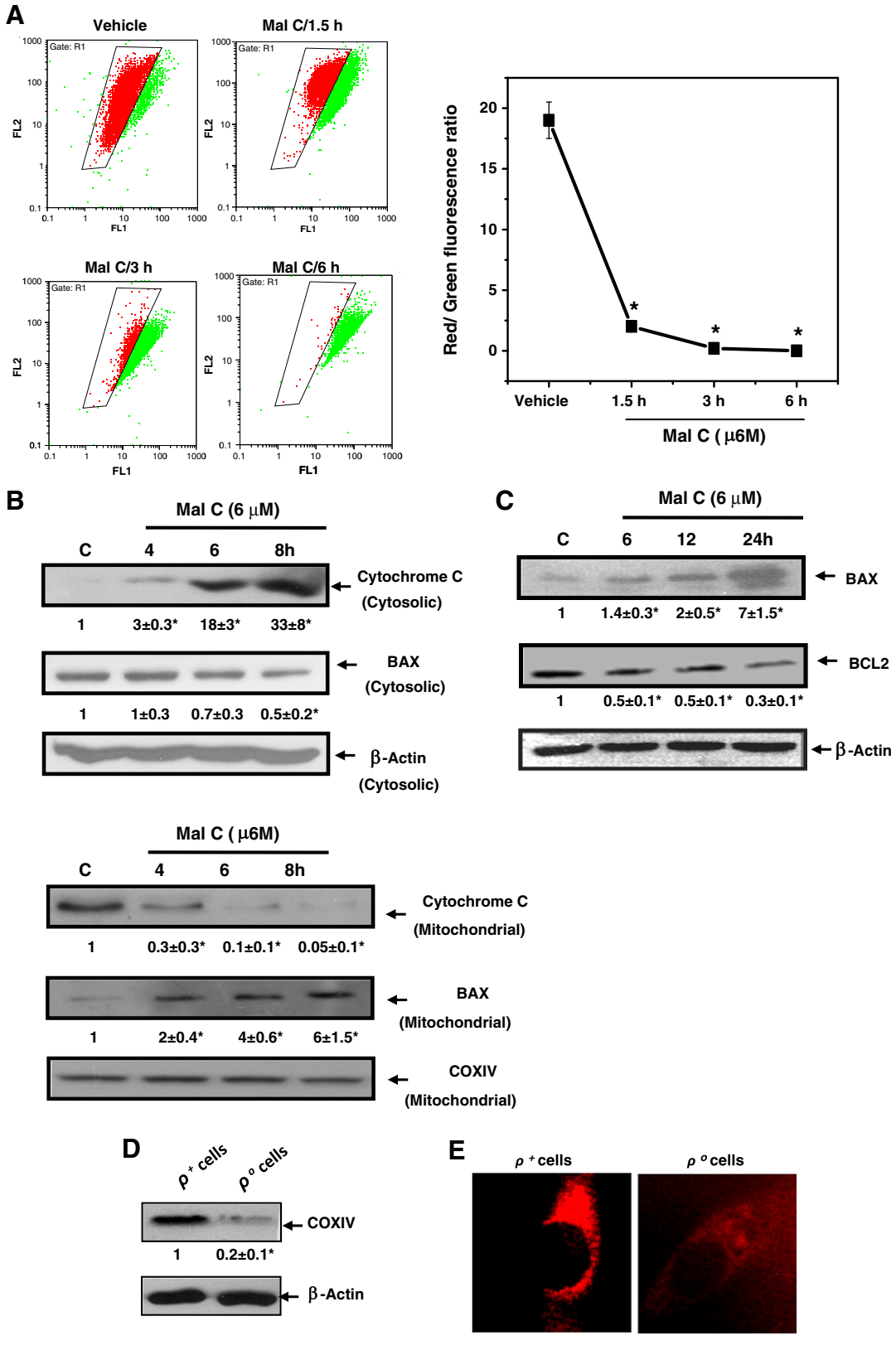

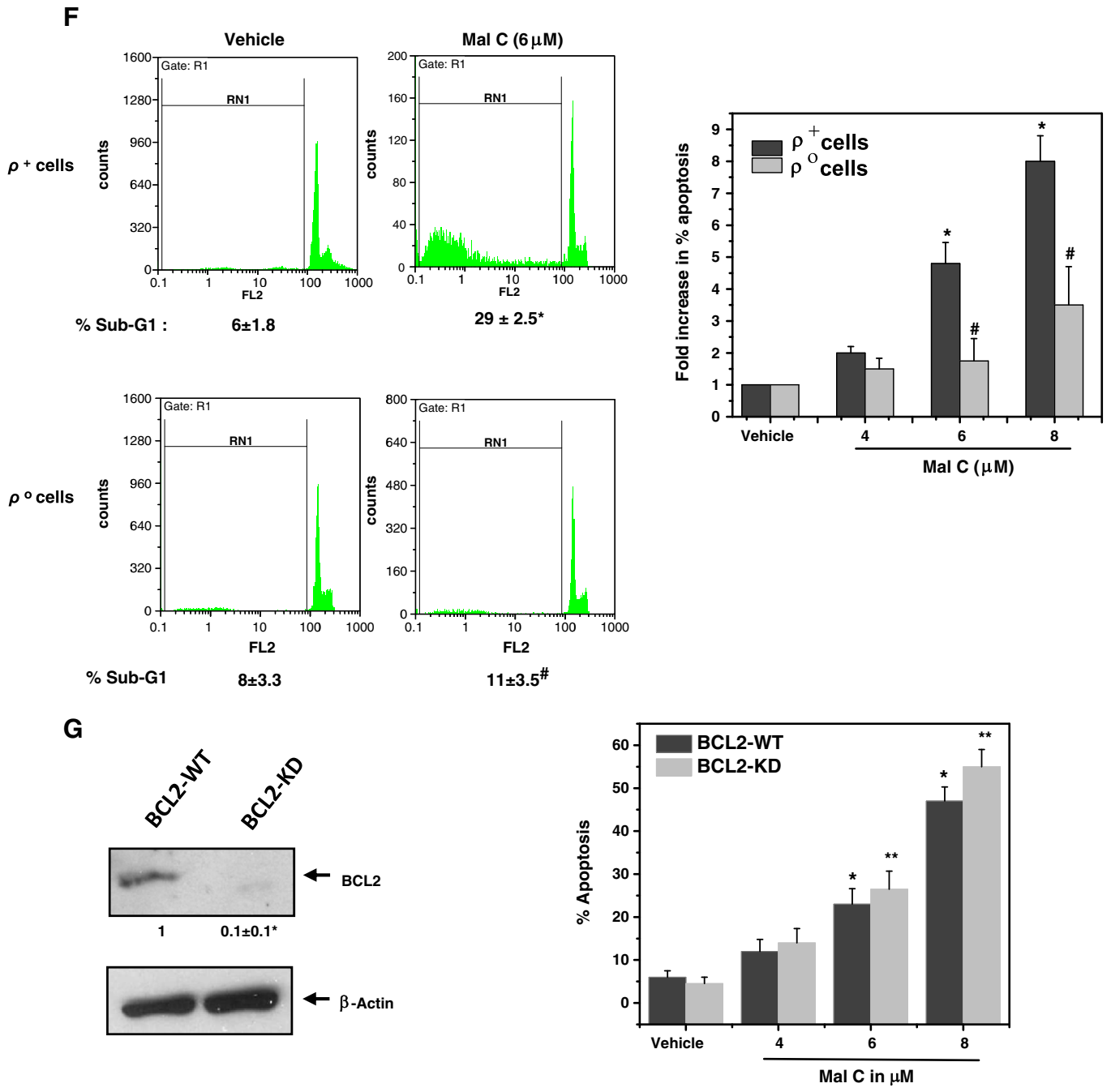

Fig. 2. Mal C-induced mitochondrial dysfunction is mediated through BAX/BCL-2 imbalance and cytochrome c release. (A) Mal C-induced $\Delta\psi_m$ loss. Cells (1×10^5 cells/well) were incubated with vehicle or mal C (6 μM) for different time periods. The cells were treated with JC-1 during the last 30 min of the mal C treatment, and $\Delta\psi_m$ were determined by flow cytometry from the retention of the red fluorescence due to JC-1 aggregates (upper panel). Simultaneously, the $\Delta\psi_m$ loss was also determined by measuring the JC-1 monomer (green fluorescence). The ratio of red/green fluorescence was quantified and shown in the lower panel. The abbreviations FL1 and FL2 in the dot plot represent intensities of the green and red fluorescences of JC-1, acquired in the channel 1 and channel 2 respectively. (B, C) Translocation and expressions of mitochondrial dysfunction-related proteins. The cells were treated with vehicle or mal C (6 μM) for different time periods. The expressions of the proteins in the cytosolic, mitochondrial and whole cell extracts were assessed by immunoblots. (D, E) Mitochondria deficiency in A549-ρ^o cells, as assessed by COX IV immunoblot and fluorescence intensity after labelling with MitoTracker red in the A549-ρ^+ and A549-ρ^o cells. (F) Concentration-dependent effect of mal C in apoptosis induction in A549-ρ^+ and A549-ρ^o cells. Cells were treated with increasing concentration of mal C and the sub-G1 population was assessed by flow cytometry. (G) Effect of mal C in apoptosis induction in BCL2 down-regulated cells. Panel 1: Confirmation of BCL2 depletion in BCL2-KD cells by immunoblot. Panel 2: The BCL2-WT and BCL2-KD cells were treated with increasing concentration of mal C and the sub-G1 population assessed by flow cytometry. All these experiments were repeated three to four times with similar results, and the values are mean ± S. E. M. $^*P < 0.01$ compared to vehicle control, $^{**}P < 0.05$, $^{\#}P < 0.01$ compared to respective mal C treatment. The images shown are representatives.

with the pan caspase inhibitor (20 μM) prior to mal C (8 μM) treatment reduced the sub-G1 cell population (~31%, $P < 0.01$), compared to the only mal C-treated cells (~47%, $P < 0.01$) (Supplementary Fig. SL6). All these results confirmed that the cytotoxicity of mal C follows an apoptotic pathway through the activation of caspases-9 and -3 as an early event, and of caspase-8 later.

3.2. Mal C perturbs mitochondrial function through BAX/BCL-2 imbalance

To determine whether mitochondrial pathway is involved in the above process, we examined mal C-induced changes in $\Delta\Psi_m$ and release of pro-apoptotic molecules from the mitochondria into cytosol. As shown in Fig. 2A and B, mal C induced significant loss of $\Delta\Psi_m$ and

release of cytochrome c into cytosol. The kinetic analysis revealed that the $\Delta\Psi_m$ loss (within 1.5 h) preceded the cytochrome c release (4 h) in response to mal C treatment, indicating an initial role of mitochondrial dysfunction in the mal C-induced cell death. Because the apoptotic BCL-2 family members, especially BAX and BCL-2 are crucial to the mitochondrial cell death pathway [10], we also analyzed the BAX and BCL-2 expressions in the mal C-treated cells. Within 6 h of treatment, mal C markedly increased the BAX expression (1.4 fold, $P < 0.001$) and its translocation to mitochondria with simultaneous reduction in BCL-2 (0.5 fold, $P < 0.001$) expression (Fig. 2B and C).

To further demonstrate the critical role of mitochondria, we analyzed the apoptosis induction in the wild type A549 cells (A549-ρ^+ cells) and in partially mitochondrial DNA depleted A549 cells (A549-ρ^o cells). The A549-ρ^o cells were characterized by the reduced (~82%) expression of the mitochondria-specific protein, COX IV that is an essential component of the mitochondrial respiratory chain (Fig. 2D). Moreover, mitochondria-specific fluorescence staining by the MitoTracker® dye showed severe loss of mitochondria in A549-ρ^o cells vis-à-vis the A549-ρ^+ cells (Fig. 2E). Flow cytometry analysis revealed that the A549-ρ^o cells were markedly resistant to mal C compared to the A549-ρ^+cells (Fig. 2F). Furthermore, shRNA-mediated depletion of the anti-apoptotic BCL-2 protein partially sensitized cell death in response to mal C treatment (Fig. 2G). These findings provide direct evidence of the essential role of mitochondria in the mal C-induced apoptosis.

3.3. P38 MAPK is an important mediator in the mal C-mediated mitochondrial dysfunction and cell death

Treatment of the A549 cells with mal C (6 μM) resulted in a marked increase in the phosphorylated forms of all three MAPKs (p38, JNK and ERK), indicating their activation (Fig. 3A). To investigate the role of individual MAPKs activation, the effects of specific inhibitors such as SB203580 (p38 inhibitor), U0126 (ERK 1/2 inhibitor), and SP600125 (JNK inhibitor) in the mal C-induced apoptosis were studied. Initially, we examined the efficacies of the p38 and JNK inhibitors in inhibiting the respective MAPKs at 3 h, as the levels of phospho-p38, and phospho-JNK were reduced at a later time point (6 h). For the ERK inhibitor, this was carried out at 6 h. Furthermore, the effects of the inhibitors on the respective downstream targets of p38 and JNK, such as MAPK activated protein kinase (MAPKAPK) and c-JUN were also investigated. Normally, p38, JNK and ERK have very low autophosphorylating activity, and their activation is presumed to be dependent mainly on upstream MAPK kinases (MAPKKs) and other kinases [24]. The inhibitors for ERK (U0126), JNK (SP600125) and p38 (SB203580) are known to inhibit the upstream kinases and/or autophosphorylation of the respective MAPKs [24–26]. In our results, the inhibitors for p38 and JNK partially inhibited the p38 and JNK phosphorylation, induced by mal C alone (Supplementary Fig. SL7). Further, mal C induced significant phosphorylations of MAPKAPK and c-JUN, which were brought down to the normal levels by these inhibitors (Supplementary Fig. SL7). On the other hand, U0126 completely suppressed the endogenous and mal C-induced phosphorylation of ERK (Supplementary Fig. SL7). This is possibly due to direct inhibition of upstream MAPKK family members, MEK-1 and MEK-2 by U0126, as reported earlier [26].

Amongst the inhibitors, only SB203580 markedly reduced the mal C-induced apoptosis (Fig. 3B), indicating the involvement of activated p38 MAPK in the process. Interestingly, the mal C-induced p38 MAPK phosphorylation was not affected in the A549-ρ^o and BCL-2 KD cells vis-à-vis the wild type cells (Fig. 3C). However, pre-treatment of p38 MAPK inhibitor abrogated the mal C-induced $\Delta\Psi_m$ loss partially (Supplementary Fig. SL8) and cytochrome c release into cytosol (Fig. 3D). Taken together, these results indicated that p38 activation is the initial event that triggers mitochondrial dysfunction in the mal C-induced cell death.

3.4. Mal C binds to DNA and induces DSBs

The DNA repair and replication machinery are known to convert SSBs into the most severe and lethal DSBs, which are powerful apoptosis inducers [27]. Earlier, mal C was found to bind with DNA in vitro through minor groove as well as intercalation, and induce SSBs in MCF7 cells [18]. To decipher the initial molecular targets of mal C, the DNA binding and damaging ability of mal C in the A549 cells were confirmed. Pre-treatment with mal C reduced the binding of a known DNA binder, Hoechst 33342 (Fig. 4A) concentration dependently. The neutral comet analysis showed no or smaller comet tail in the untreated cells, while mal C dose-dependently induced longer comet tails in the cells (Fig. 4B). In corroboration with these results, the level of the DSB marker, phosphorylated H2AX (γH2AX) was also increased in response to mal C treatment (Fig. 4C). The DNA DSB was not induced up to 1 h of mal C treatment, but cells with significantly larger tails were seen after 2 h (data not shown).

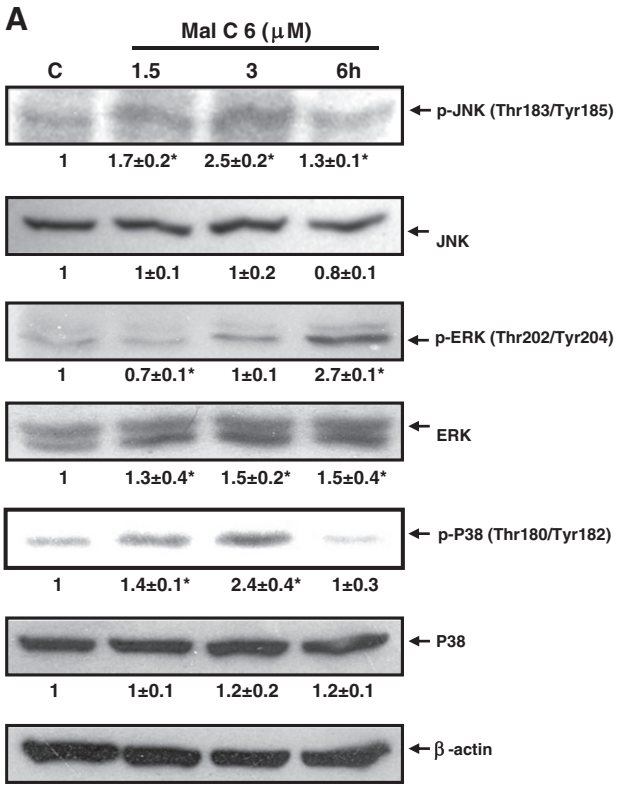

Fig. 3. p38 MAPK acts as a critical upstream mediator in mal C-induced mitochondrial cell death. (A) MAPKs activation. A549 cells were treated with mal C (6 μM) for different time periods. The MAPKs activation was assessed by immunoblots of the respective phosphorylated proteins in the cell lysates. The experiments were repeated three times with similar results, and representative images are shown. $^*P < 0.05$ compared to vehicle control. (B) Effect of MAPK inhibitor in mal C induced apoptosis. Cells were pretreated with different MAPK specific inhibitors (each 25 μM) and referred as p38*i*, JNK*i* and ERK*i* cells. Subsequently the cells were incubated with different concentrations of mal C for 24 h and the sub-G1 population was assessed by flow cytometry. The abbreviation FL2 in the histogram represents intensity of the red fluorescence of propidium dye, acquired in channel-2. The experiments were repeated four times with similar results. All determinations were made in three replicates, and the mean values are shown. (C) p38 activation in A549-ρ^+, A549-ρ^o, BCL2-WT and BCL2-KD cells. Respective cells were incubated with vehicle alone or mal C (4 and 6 μM) for 3 h and the phospho-p38 (p-p38) levels in the cell lysates were assessed by immunoblots. The experiments were repeated three times with similar results, and representative images are shown. $^*P < 0.05$ compared to respective vehicle control. (D) Effect of p38 inhibitor on cytochrome c release. The SB203580-pretreated cells were exposed to mal C for 3 h and the cytochrome c release into cytoplasm was analyzed by immunoblots. The experiments were repeated three times with similar results, and representative images are shown. $^*P < 0.05$ compared to vehicle control, $^{\#}P < 0.05$ compared to only mal C treatment.

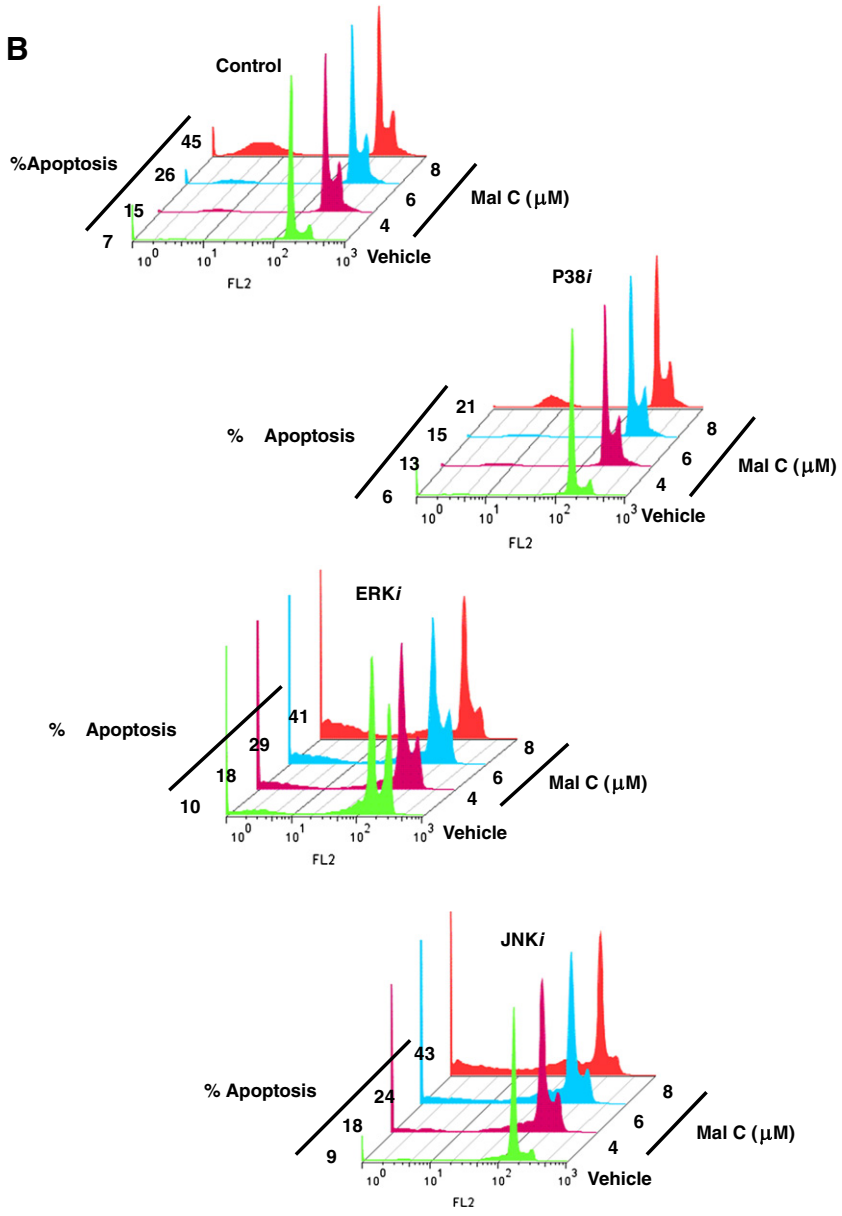

Fig. 3 (*continued*).

3.5. Mal C induces ATM/ATR-mediated DNA damage response and p38 MAPK activation

Based on the above results, we hypothesized that the mal C-induced DSBs and putative DNA damage response could lead to the p38 MAPK activation and subsequent mitochondrial death. The ATM and ATR kinases play distinct, but overlapping roles in response to DNA DSBs [20]. To substantiate the hypothesis, auto-phosphorylation at Ser-1981 ATM, and ATR-mediated Ser-345 phosphorylation in CHK1 protein were analyzed. As shown in Fig. 5A, mal C (6 μM, 3 h)-treatment not only increased phosphorylation of H2AX, but also induced a significant amount of phosphorylation on ATM-Ser1981 and CHK1-Ser345 (Fig. 5A). This suggested a rapid activation of DNA damage response pathway in cancer cells by mal C treatment.

Next we determined whether down-regulation of ATM or ATR in the A549 cells impacts p38 MAPK response following mal C treatment. For this, the ATM-depleted cells were generated using ATM mRNA specific shRNA (Fig. 5B). As ATR is an essential gene, and stable ATR-knockdown cells are not viable, we used schisandrin B, a known ATR-specific inhibitor to obtain the ATR*i* cells [28]. Next, the activation of ATM and ATR as well as p38 MAPK pathways in ATM-WT (scrambled shRNA control), ATM-KD (ATM shRNA) and ATR*i* cells was evaluated. Mal C (6 μM) markedly induced phosphorylation of ATM, CHK1, H2AX and p38 in ATM-WT cells (Fig. 5B), suggesting that both ATM and ATR pathways are activated in response to mal C treatment. However, compared to the wild type cells, phosphorylation of CHK1, H2AX and p38 MAPK was significantly reduced in the ATM-KD as well as ATR*i* cells. It is imperative to note that phosphorylation of CHK1, a downstream target of ATR was also abrogated in the ATM-KD cells. Altogether these results suggested a predominant role of both ATM and ATR pathways in p38 MAPK activation by mal C.

3.6. Inhibition of ATM, ATR or CHK1 proteins leads to abrogation of mal C-induced apoptosis

To probe the participation of ATM-CHK1 in p38 MAPK activation and mitochondrial dysfunction, the p38 MAPK phosphorylation and mitochondrial cytochrome c release in the mal C-treated ATM-WT, ATM-KD and CHK1*i* cells were assessed. ATM down regulation as well as CHK1 inhibition markedly reduced p38 phosphorylation and

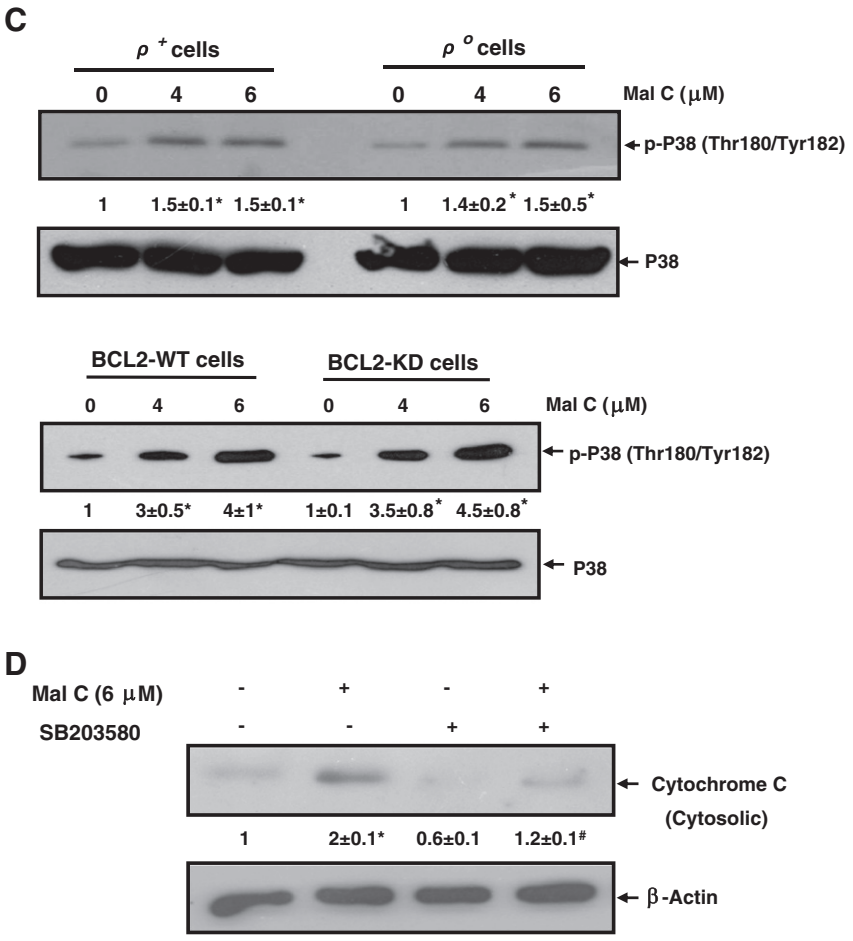

Fig. 3 (*continued*).

mitochondrial release of cytochrome c in the ATM-KD and CHK1*i* cells vis-a-vis the ATM-WT cells (Fig. 6A). Furthermore, the mal C-induced apoptosis was significantly reduced in CHK1*i* and ATM*i* cells (Fig. 6B), although the ATR inhibitor offered only a marginal protection. These results unraveled the hierarchy of molecular events in which ATM regulates the MAPK cascade that leads to cell death in the mal C-treated A549 cells.

4. Discussion

Although mal C has been recently shown to induce viability loss in certain cancer cells, the mechanism of cell death is largely unknown. Our initial MTT assay results revealed mal C to be a more potent antiproliferative agent than curcumin in multiple lung cancer cell lines. Further, amongst the known natural malabaricones, mal C showed the best anti-cancer activity against the A549 cells. The efficacy of mal C was marginally higher in A549 (IC50 7.0 ± 1.8 μM) and NCI-H460 (IC50 7.7 ± 2.1 μM) cells than NCI-H23 cells (IC50 9.9 ± 2.7 μM) (Supplementary Fig. SL2). The marginal resistance offered by NCI-H23 cells, in response to mal C may be due to its low cellular uptake, the known *p53* mutated status of the NCI-H23 cells and other genotypic modifications. We show that mal C induces mitochondria-mediated cell death that requires DNA damage-dependent activation of both CHK1 and p38 MAPK.

Many studies have demonstrated that apoptosis induction plays the most vital role in the cancer treatment by chemo- and radiation therapies [29]. Here we established that the mal C-mediated cell viability loss of A549 cells is related to apoptosis induction, as it induced (a) rapid translocation of PS from the inner to the outer leaflet of the plasma membrane, an early marker of apoptosis (Supplementary Fig. SL4); (b) histone release, DNA fragmentation (Supplementary Fig. SL5) and generation of sub-G1 particles (Fig. 1C), reflecting the late stage of apoptosis; (c) caspases-3, -8, and -9 activities, which were inhibited by the respective specific inhibitors (Fig. 1D); and (d) cleavage of procaspases -3, -8 and -9 (Fig. 1E).

The mal C-mediated apoptosis in the A549 cells was also accompanied by rapid collapse of MTP, leading to the release of apoptogenic molecule, cytochrome c from the mitochondria to the cytosol. However, it did not induce any cytochrome c release in normal HEK 293 cells (data not shown), suggesting its non-toxicity to human normal cells. The antiapoptotic BCL-2 family members (BCL-2 and BCL-xL) play an important role in the regulation of mitochondria-mediated apoptosis by different stimuli [30]. These antiapoptotic proteins possess four conserved BCL-2 homology domains (BH1–BH4), and mainly prevent the release of apoptogenic molecules (e.g. cytochrome c) from mitochondria to the cytosol by forming heterodimer complexes with the proapoptotic family members such as BAX [30–32]. Increased expression of BCL-2 has been observed in a variety of hematologic malignancies and solid tumors, and its overexpression renders cancer cells resistant to different apoptotic stimuli including the chemotherapeutic agents [32]. Mal C treatment selectively and differentially regulated the anti- and pro-apoptotic BCL-2 proteins to ameliorate apoptotic stimuli. It induced a time-dependent decrease in BCL-2 level, while augmenting BAX level in the A549 cells. The mitochondria-depleted A549-ρ^o cells were extremely resistant to mal C treatment (Fig. 2F), but BCL-2 depletion conferred partial sensitization in the A549 cells to mal C (Fig. 2G). Nevertheless, a decisive role of mitochondria in mal C-induced apoptosis was inferred from these results.

Earlier, the MAPK proteins, especially JNK and p38 were suggested to activate caspases through modulating BAX, BCL-2, and mitochondrial dysfunction to execute apoptosis [7,8]. We also found mal C-induced rapid activation of JNK and p38 in the A549 cells, while ERK was activated much later (Fig. 3A). The observed dephosphorylation of the p38 and JNK proteins at a longer time point (6 h) may be due to the activation of dephosphorylating phosphatases [33]. Nevertheless, besides its transcriptional effects, transient MAPKs activation is sufficient to regulate cell behavior, as it can induce phosphorylation of the cytoplasmic target proteins, such as the apoptotic (e.g., BH3-only family) proteins [33–35]. However, currently we do not have any evidence to suggest the exact mechanism of dephosphorylation of activated MAPKs and further activation of specific downstream apoptotic targets during later time point of mal C treatment.

Our studies with specific MAPKs inhibitors, carried out at 3 h (when p38 and JNK are robustly activated) revealed partial inhibition of mal C-induced p38 and JNK phosphorylation. This suggested that SB203580 and SP600125 may be inhibiting the autophosphorylation of p38 and JNK, but not their phosphorylation by the upstream kinases. Moreover, the respective inhibitors also restored the normal levels of MAPKAPK and c-JUN, the downstream targets of p38 and JNK in the mal C-treated cells, without showing any effect on their own. All these results confirmed the efficacies of the chosen inhibitors. Overall, the above results suggested that these MAPKs inhibitors can inhibit upstream kinases or autophosphorylation of MAPKs to effectively abrogate further downstream signaling of p38, JNK and ERK in response to mal C treatment.

Amongst the MAPK inhibitors, only the p38-specific inhibitor reduced the mal C-mediated apoptosis in the cells (Fig. 3B). Further, mal C increased the p38-phosphorylation almost equally in the A549-ρ^+/A549-ρ^o and BCL2-WT/BCL2-KD cells (Fig. 3C), and inhibition of p38 MAPK partially attenuated the mal C-induced $\Delta\Psi_m$ loss (Supplementary Fig. SL8) and cytochrome c release in the cytosol (Fig. 3D). These implied a major role of p38 MAPK activation in the upstream, but not on the downstream in the mitochondrial damage.

Intracellular ROS accumulation has been shown to cause $\Delta\Psi_m$ loss, mitochondrial membrane permeability transition and subsequent activation of cell death machinery [36]. Recent studies also provide evidence for the role of ROS as the potential inducers of MAPK activation during apoptotic cell death in response to a variety of different stimuli [36–38]. Previously, we have shown that mal C generates ROS in a cell free system [18]. Interestingly however, pretreatment of the A549 cells with NAC, a known antioxidant did not impede mal C-induced p38 MAPK phosphorylation (data not shown), excluding any direct role of ROS in the cytotoxicity of mal C. It is of future interest to determine whether ROS is required to potentiate some of the mal C-mediated processes to ameliorate apoptosis process under specific conditions. It is worth mentioning that mal B, the structural congener of mal C also induced copious ROS generation, and its abrogation with NAC drastically reduced the sensitivity of the A549 cells towards mal B.

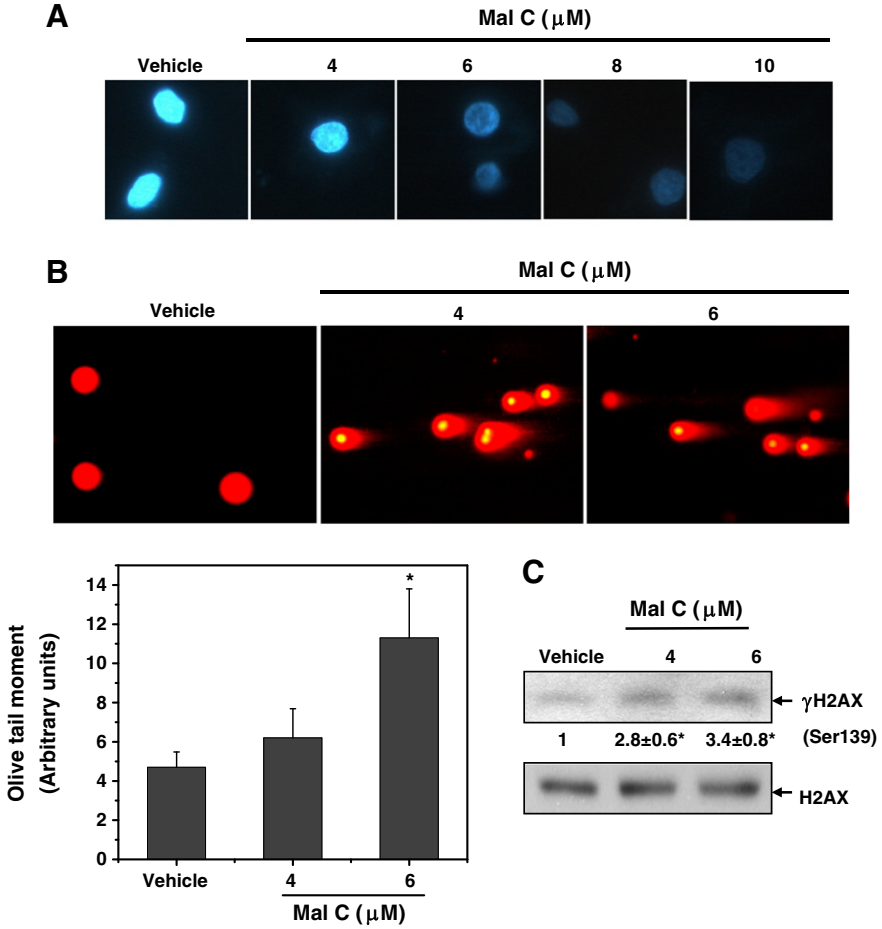

Fig. 4. Mal C binds DNA and induces DNA DSBs. (A) DNA binding. The A549 cells were treated with different concentrations of mal C for 1 h. After washing off mal C, cells were labeled with Hoechst 33342, and visualized under an inverted fluorescent microscope. (B) DNA DSB analysis. Upper panel: Olive tails. Lower panel: Quantification of the olive tail moment from the above experiments. (C) γH2AX formation. The A549 cells were treated with vehicle alone or different concentrations of mal C for 3 h. The DNA DSB was assessed by neutral comet assay, while γH2AX was analyzed by immunoblots of the cell lysates. All the experiments were repeated three times with similar results. All determinations were made in three replicates, and the values are means ± S. E. M. $^*P < 0.01$ compared to vehicle control. Representative images are shown.

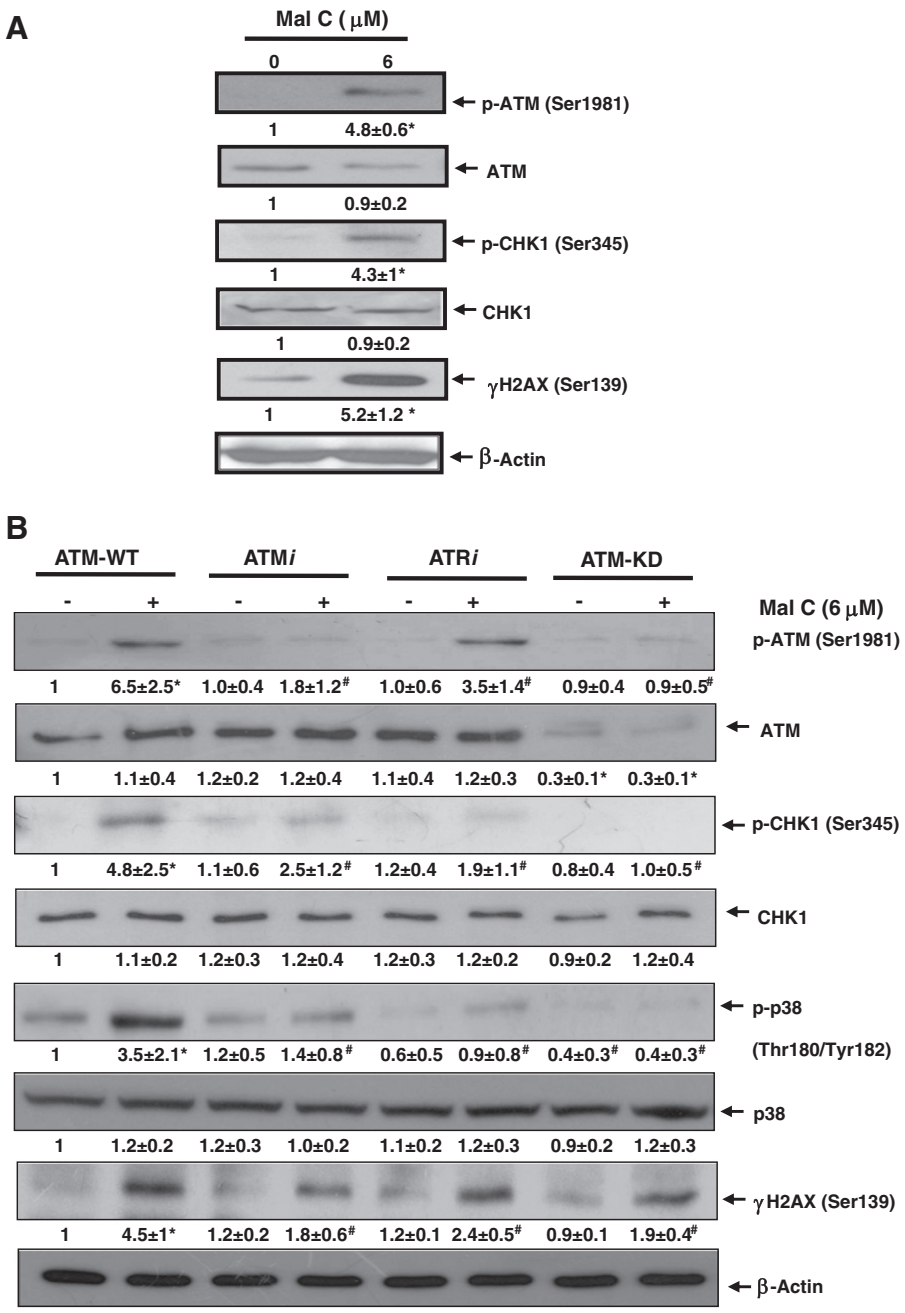

Fig. 5. Mal C elicits ATM/ATR mediated p38 MAPK activation in response to DNA damage. (A) Phosphorylation levels of ATM, CHK1 and H2AX. The A549 cells were treated with vehicle alone or mal C (6 μM) for 3 h and the cell lysates were analyzed for the phosphorylation levels of respective proteins by immunoblots. (B) Effect of ATM and ATR downregulation. The ATM-WT, ATM*i*, ATR*i* and ATM-KD cells were treated with vehicle alone or mal C (6 μM) for 3 h and the cell lysates were analyzed for p-ATM, p-CHK1, p-p38 and γH2AX by immunoblots. For ATM*i* and ATR*i*, the respective specific inhibitors, KU55933 (10 μM) and schisandrin B (25 μM) were used. The experiments were repeated three times with similar results, and representative images are shown. $^{*}P < 0.05$ compared to vehicle control, $^{\#}P < 0.05$ compared to mal C-treated ATM-WT cells.

This suggested that the mal B-induced apoptosis followed the conventional ROS-mediated pathway.

The canonical DNA damage response (DDR) network can be divided into two major protein kinases signaling branches, which mediate checkpoint activation through the upstream kinases, ATM-CHK2 and ATR-CHK1, respectively [39–42]. A third checkpoint effector pathway, mediated by p38 and MAPKAP kinase-2 (MK2) operates parallel to CHK1, and is activated downstream of ATM and ATR [43–45]. The DDR-mediated sustained activation of p38 and JNK is responsible for the cisplatin-induced apoptosis via activation of the death receptor pathway [46,47]. Also, down-regulation of the CDC7 kinase activity induced ATR-mediated p38 activation to execute apoptosis in human cancer cells [12]. Because mal C induced DNA SSBs in MCF7 breast cancer cells, we hypothesized that a similar mal C-mediated SSBs in A549 cells might be converted into DSBs due to the replication and/or DNA damage repair pathways. This may activate p38 MAPK. Results (Fig. 4A and B) of our neutral comet and γH2AX assay showed that mal C binds to nuclear DNA effectively, and induces DSBs concentration-dependently. Furthermore, mal C also activated the DDR response proteins ATM and ATR by inducing rapid autophosphorylation at Ser-1981 in ATM and phosphorylation of Ser-345 in CHK1 (Fig. 5A).

The shRNA mediated silencing of ATM or ATR inhibition led to a significant reduction in p38 MAPK phosphorylation (Fig. 5B), suggesting a

predominant, but redundant role of the ATM and ATR pathways in p38 MAPK activation. Intriguingly we also noticed that the mal C-induced phosphorylation of CHK1, generally an ATR target, is also partially abrogated in the ATM knock-down cells. Consistent with this, CHK1 inhibition completely abrogated the mal C-mediated p38 phosphorylation and cytochrome c release from mitochondria (Fig. 6A). However, the mal C-induced γH2AX formation and CHK1 phosphorylation was not affected by the p38 MAPK inhibitor (data not shown). From this, a pivotal upstream role of the ATM/ATR-CHK1 pathway in the p38-mediated apoptosis was inferred. Although the ATM-CHK1 pathway is not activated regularly, involvement of this unscrupulous pathway in response to radiation and certain other DNA damaging agents is reported [48,49].

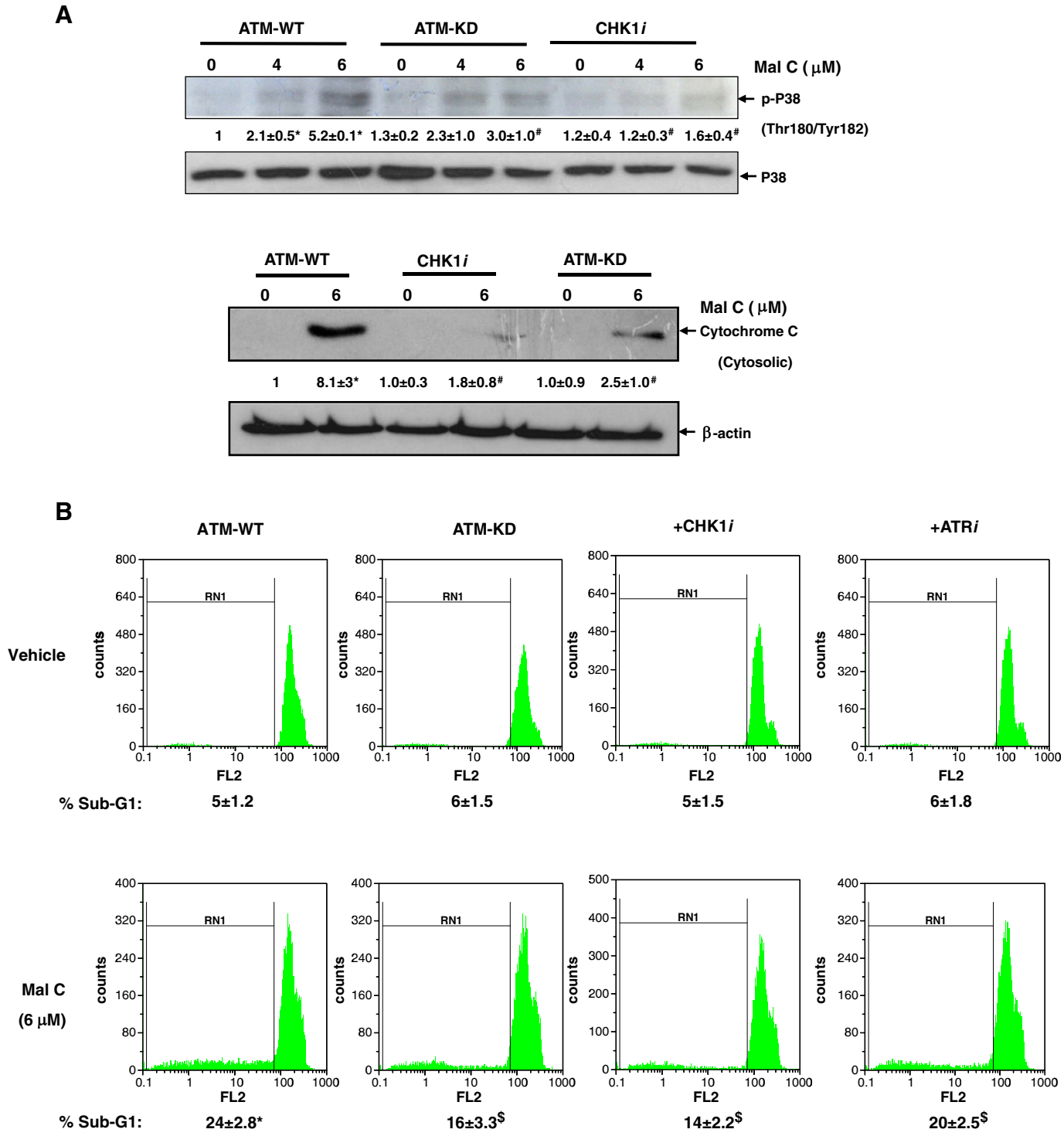

Fig. 6. Inhibition of ATM, ATR or CHK1 proteins leads to abrogation of mal C-induced apoptosis. (A) Effect of ATM and CHK1 on p38 phosphorylation and cytochrome c release from mitochondria. The ATM-WT, ATM-KD and CHK1*i* cells were treated with vehicle alone or different concentrations of mal C and the p-p38 levels in the cell lysates and cytochrome c release into cytosol were analyzed by immunoblots. (B) Effect of ATM, ATR or CHK1 on apoptosis induction. The ATM-WT, ATM-KD, ATR*i* and CHK1*i* cells were treated with vehicle alone or mal C (6 μM) for 24 h and the sub-G1 populations were assessed by flow cytometry. For ATR*i* and CHK1*i*, the respective specific inhibitors, schisandrin B (25 μM) and UCN-01 (100 nM) were used. The abbreviation FL2 in the histogram represents intensity of the red fluorescence of propidium dye, acquired in channel-2. The experiments were repeated four times with similar results. All determinations were made in three replicates, and the values are means ± S. E. M. $^{*}P < 0.01$ compared to vehicle control, $^{\$}P < 0.05$, $^{\#}P < 0.01$ compared to mal C-treated ATM-WT cells.

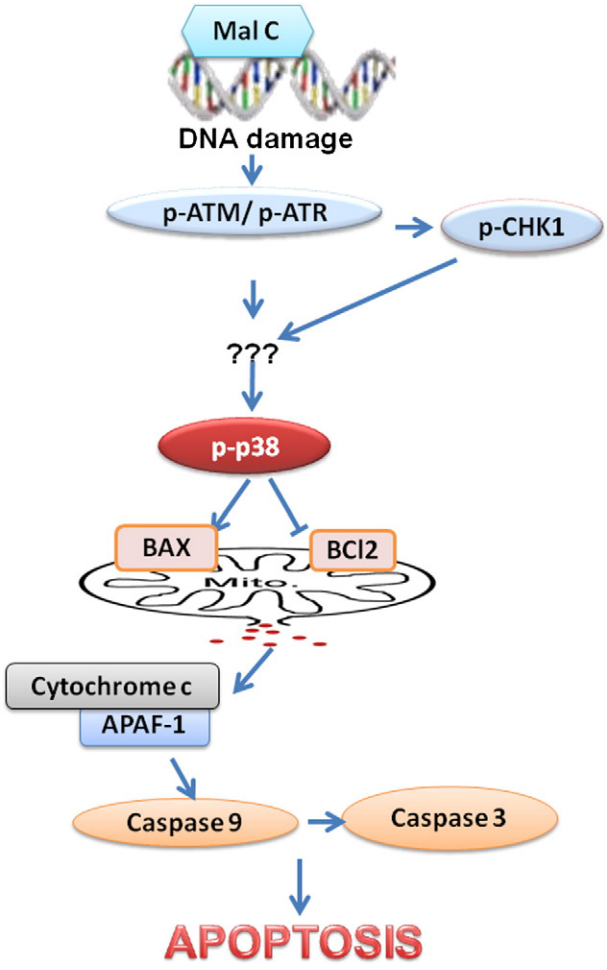

Fig. 7. Possible molecular mechanism of mal C-induced cell death in the A549 cells.

Overall, ATM down-regulation or inhibition of CHK1 and ATR greatly attenuated the killing effect of mal C. This is compatible with the model that mal C induces DSB via the ATM/ATR-CHK1 pathway, which activates p38 to trigger apoptosis through mitochondrial damage (Fig. 7). ATM, ATR and CHK1 kinases are known to regulate the phosphorylation of consensus sequence serine and threonine followed by glutamine (S/T-Q sites), while p38 MAPK activation occurs through the dual phosphorylation on a tyrosine residue of T–X–Y motif in the activation loop [50]. This suggests that ATM-CHK1 kinases are not directly involved in the phosphorylation of p38 MAPK, but possibly through the activation of some other potential tyrosine phosphorylating kinase/s. It is tempting to speculate that mal C-induced ATM/ATR-CHK1 pathway might be involved in the activation of some of the upstream MAPKKKs known to participate in the activation of the p38 MAPK cascade including MEKK1/4, ASK1, and TAO kinases [50]. Further systematic studies are needed to explore this possibility.

In conclusion, mal C showed significant potential as a therapeutic agent against human lung cancer (especially A549) cell lines. Initially mal C induces DSB-DNA in the A549 cells, which induces p38 MAPK activation, Bax translocation, mitochondrial membrane potential collapse, caspase-3 activation and eventual cell death. A mechanistic model, explaining the mode of action of mal C is shown in Fig. 7.

Appendix A. Supplementary data

Supplementary data to this article can be found online at http://dx.doi.org/10.1016/j.bbagen.2013.11.020.

References

[1] C.G. Slatore, M.K. Gould, D.H. Au, M.E. Deffebach, E. White, Lung cancer stage at diagnosis: individual associations in the prospective VITamins and lifestyle (VITAL) cohort, BMC Cancer 11 (2011) 228.
[2] I.R. Indran, G. Tufo, S. Pervaiz, C. Brenner, Recent advances in apoptosis, mitochondria and drug resistance in cancer cells, BBA — Bioenerg. 6 (2011) 735–745.
[3] A.K. Maity, Reactive oxygen species reduction is a key underlying mechanism of drug resistance in cancer chemotherapy, Chemotherapy 1 (2012) 104.
[4] J.Y. Byun, M.J. Kim, D.Y. Eum, C.H. Yoon, W.D. Seo, K.H. Park, J.W. Hyun, Y.S. Lee, J.S. Lee, M.Y. Yoon, S.J. Lee, Reactive oxygen species-dependent activation of bax and poly (ADP-ribose) polymerase-1 is required for mitochondrial cell death induced by triterpenoid pristimerin in human cervical cancer cells, Mol. Pharmacol. 76 (2009) 734–744.
[5] Z. Huang, A. Tunnacliffe, Response of human cells to desiccation: comparison with hyperosmotic stress response, J. Physiol. 558 (2004) 181–191.
[6] X. Li, R. Zhang, D. Luo, S.J. Park, Q. Wang, Y. Kim, W. Min, Tumor necrosis factor alpha-induced desumoylation and cytoplasmic translocation of homeodomain interacting protein kinase 1 are critical for apoptosis signal-regulating kinase 1-JNK/p38 activation, J. Biol. Chem. 280 (2005) 15061–15070.
[7] Y.H. Kang, S.J. Lee, The role of p38 MAPK and JNK in Arsenic trioxide induced mitochondrial cell death in human cervical cancer cells, J. Cell. Physiol. 217 (2008) 23–33.
[8] M.J. Kim, S.Y. Choi, I.C. Park, S.G. Hwang, C. Kim, Y.H. Choi, H. Kim, K.H. Lee, S.J. Lee, Opposing roles of c-Jun NH2-terminal kinase and p38 mitogen-activated protein kinase in the cellular response to ionizing radiation in human cervical cancer cells, Mol. Cancer Res. 6 (2008) 1718–1731.
[9] S.Y. Choi, M.J. Kim, C.M. Kang, S. Bae, C.K. Cho, J.W. Soh, J.H. Kim, S. Kang, H.Y. Chung, Y.S. Lee, S.J. Lee, Activation of bak and bax through c-abl-protein kinase C delta-p38 MAPK signaling in response to ionizing radiation, J. Biol. Chem. 281 (2006) 7049–7059.
[10] A.B. Gustafsson, R.A. Gottlieb, Bcl-2 family members and apoptosis, taken to heart, Am. J. Physiol. Cell Physiol. 292 (2007) C45–C51.
[11] D. Selimovic, M. Hassan, Y. Haikel, U.R. Hengge, Taxol-induced mitochondrial stress in melanoma cells is mediated by activation of c-Jun N-terminal kinase (JNK) and p38 pathways via uncoupling protein 2, Cell. Signal. 20 (2008) 311–322.
[12] J.S. Im, J.K. Lee, ATR-dependent activation of p38 MAP kinase is responsible for apoptotic cell death in cells depleted of Cdc7, J. Biol. Chem. 283 (2008) 25171–25177.
[13] V. Palani, R.K. Senthilkumaran, B.S. Govindasamy, Biochemical evaluation of antitumor effect of MuthuMarunthu (a herbal formulation) on experimental fibrosarcoma in rats, J. Ethnopharmacol. 65 (1999) 257–265.
[14] K.R. Kirtikar, B.D. Basu, Indian medicinal plants, Periodical Experts, vol. 1, Jayyed Press, Delhi, 1975.
[15] B.S. Patro, A.K. Bauri, S. Mishra, S. Chattopadhyay, Antioxidant activity of *Myristica malabarica* extracts and their constituents, J. Agric. Food Chem. 53 (2005) 6912–6918.
[16] D. Banerjee, A.K. Bauri, R.K. Guha, S.K. Bandyopadhyay, S. Chattopadhyay, Healing properties of malabaricone B and malabaricone C against indomethacin-induced gastric ulceration and mechanism of action, Eur. J. Pharmacol. 578 (2008) 300–312.
[17] B. Maity, S.K. Yadav, B.S. Patro, M. Tyagi, S.K. Bandyopadhyay, S. Chattopadhyay, Molecular mechanism of the anti-inflammatory activity of a natural diarylnonanoid, malabaricone C, Free Radic. Biol. Med. 52 (2012) 1680–1691.
[18] B.S. Patro, M. Tyagi, J. Saha, S. Chattopadhyay, Comparative nuclease and anti-cancer properties of the naturally occurring malabaricones, Bioorg. Med. Chem. 18 (2010) 7043–7051.
[19] K.K. Purushothaman, A. Sarada, J.D. Connolly, Malabaricones A–D, novel diarylnonanoids from *Myristica malabarica* Lam (*Myristicaceae*), J. Chem. Soc. Perkin Trans. 15 (1977) 587–588.
[20] B.S. Patro, R. Frøhlich, V.A. Bohr, T. Stevnsner, WRN helicase regulates the ATR-CHK1-induced S-phase checkpoint pathway in response to topoisomerase-I–DNA covalent complexes, J. Cell Sci. 124 (2011) 3967–3979.
[21] D. Xiao, A.A. Powolny, M.B. Moura, E.E. Kelley, A. Bommareddy, S.H. Kim, E.R. Hahm, D. Normolle, H.B. Van, S.V. Singh, Phenethyl isothiocyanate inhibits oxidative phosphorylation to trigger reactive oxygen species-mediated death of human prostate cancer cells, J. Biol. Chem. 285 (2010) 26558–26569.
[22] B.S. Patro, B. Maity, S. Chattopadhyay, Topoisomerase inhibitor coralyne photosensitizes DNA, leading to elicitation of Chk2-dependent S-phase checkpoint and p53-independent apoptosis in cancer cells, Antioxid. Redox Signal. 10 (2012) 945–960.
[23] M.P. King, G. Attadi, Mitochondria-mediated transformation of human rho(0) cells, Methods Enzymol. 264 (1996) 313–334.
[24] J.M. Salvador, P.R. Mittelstadt, T. Guszczynski, T.D. Copeland, H. Yamaguchi, E. Appella, A.J. Fornace Jr., J.D. Ashwell, Alternative p38 activation pathway mediated by T cell receptor–proximal tyrosine kinases, Nat. Immunol. 6 (2005) 390–395.
[25] H. Tsuiki, M. Tnani, I. Okamoto, L.C. Kenyon, D.R. Emlet, M. Holgado-Madruga, I.S. Lanham, C.J. Joynes, K.T. Vo, A.J. Wong, Constitutively active forms of c-Jun NH2-terminal kinase are expressed in primary glial tumors, Cancer Res. 63 (2003) 250–255.
[26] M.F. Favata, K.Y. Horiuchi, E.J. Manos, A.J. Daulerio, D.A. Stradley, W.S. Feeser, D.E.V. Dyk, W.J. Pitts, R.A. Earl, F. Hobbs, R.A. Copeland, R.L. Magolda, P.A. Scherle, J.M. Trzaskos, Identification of a novel inhibitor of mitogen-activated protein kinase kinase, J. Biol. Chem. 273 (1998) 18623–18632.
[27] N. Berdelle, T. Nikolova, S. Quiros, T. Efferth, B. Kaina, Artesunate induces oxidative DNA damage, sustained DNA double-strand breaks, and the ATM/ATR damage response in cancer cells, Mol. Cancer Ther. 10 (2011) 2224–2233.
[28] H. Nishida, N. Tatewaki, Y. Nakajima, T. Magara, K.M. Ko, Y. Hamamori, T. Konishi, Inhibition of ATR protein kinase activity by schisandrin B in DNA damage response, Nucleic Acids Res. 37 (2009) 5678–5689.

[29] G.I. Evan, K.H. Vousden, Proliferation, cell cycle and apoptosis in cancer, Nature 411 (2001) 342–343.
[30] D.T. Chao, S.J. Korsmeyer, BCL-2 family: regulators of cell death, Annu. Rev. Immunol. 16 (1998) 395–419.
[31] Z.N. Oltvai, C.L. Milliman, S.J. Korsmeyer, Bcl-2 heterodimerizes in vivo with a conserved homolog, Bax, that accelerates programmed cell death, Cell 74 (1993) 609–619.
[32] A. Mazars, O. Genesto, J. Hickman, The Bcl-2 family of proteins as drug targets, J. Soc. Biol. 199 (2005) 253–265.
[33] M.R. Junttila, S. Li, J. Westermarck, Phosphatase-mediated crosstalk between MAPK signaling pathways in the regulation of cell survival, FASEB J. 22 (2008) 954–965.
[34] X. Wang, L. Cui, J. Joseph, B. Jiang, D. Pimental, D.E. Handy, R. Liao, J. Loscalzo, Homocysteine induces cardiomyocyte dysfunction and apoptosis through p38 MAPK-mediated increase in oxidant stress, J. Mol. Cell. Cardiol. 52 (2012) 753–760.
[35] H.J. Cho, S. Park, E.M. Hwang, K.E. Baek, I. Kim, I. Nam, M. Im, S. Park, S. Bae, J.Y. Park, J. Yoo, Gadd45b mediates Fas-induced apoptosis by enhancing the interaction between p38 and retinoblastoma tumor suppressor, J. Biol. Chem. 285 (2010) 25500–25505.
[36] C. Fleury, B. Mignotte, J.L. Vayssie're, Mitochondrial reactive oxygen species in cell death signalling, Biochimie 84 (2002) 131–141.
[37] M.T. Park, M.J. Kim, Y.H. Kang, S.Y. Choi, J.H. Lee, J.A. Choi, C.M. Kang, C.K. Cho, S. Kang, S. Bae, Phytosphingosine in combination with ionizing radiation enhances apoptotic cell death in radiation-resistant cancer cells through ROS dependent and independent AIF release, Blood 105 (2005) 1724–1733.
[38] M. Kuwabara, T. Asanuma, K. Niwa, O. Inanami, Regulation of cell survival and death signals induced by oxidative stress, J. Clin. Biochem. Nutr. 43 (2008) 51–57.
[39] J. Bartek, J. Lukas, Chk1 and Chk2 kinases in checkpoint control and cancer, Cancer Cell 3 (2003) 421–429.
[40] J.W. Harper, S.J. Elledge, The DNA damage response: ten years after, Mol. Cell 28 (2007) 739–745.
[41] M.B. Kastan, Q. Zhan, W.S. el-Deiry, F. Carrier, T. Jacks, W.V. Walsh, B.S. Plunkett, B. Vogelstein, A.J. Fornace Jr., A mammalian cell cycle checkpoint pathway utilizing p53 and GADD45 is defective in ataxia-telangiectasia, Cell 71 (1992) 587–597.
[42] Y. Shiloh, ATM and related protein kinases: safeguarding genome integrity, Nat. Rev. Cancer 3 (2003) 155–168.
[43] D.V. Bulavin, S. Saito, M.C. Hollander, K. Sakaguchi, C.W. Anderson, E. Appella, A.J. Fornace Jr., Phosphorylation of human p53 by p38 kinase coordinates N-terminal phosphorylation and apoptosis in response to UV radiation, EMBO J. 18 (1999) 6845–6854.
[44] I.A. Manke, A. Nguyen, D. Lim, M.Q. Stewart, A.E. Elia, M.B. Yaffe, MAPKAP kinase-2 is a cell cycle checkpoint kinase that regulates the G2/M transition and S phase progression in response to UV irradiation, Mol. Cell 17 (2005) 37–48.
[45] H.C. Reinhardt, A.S. Aslanian, J.A. Lees, M.B. Yaffe, p53-deficient cells rely on ATM- and ATR-mediated checkpoint signaling through the p38MAPK/MK2 pathway for survival after DNA damage, Cancer Cell 11 (2007) 175–189.
[46] W.P. Roos, B. Kaina, DNA damage-induced cell death by apoptosis, Trends Mol. Med. 12 (2006) 440–450.
[47] A. Mansouri, L.D. Ridgway, A.L. Korapati, Q. Zhang, L. Tian, Y. Wang, Z.H. Siddik, G.B. Mills, F.X. Claret, Sustained activation of JNK/p38 MAPK pathways in response to cisplatin leads to fas ligand induction and cell death in ovarian carcinoma cells, J. Biol. Chem. 278 (2003) 19245–19256.
[48] M. Gatei, K. Sloper, C. Sorensen, R. Syljuäsen, J. Falck, K. Hobson, K. Savage, J. Lukas, B.B. Zhou, J. Bartek, K.K. Khanna, Ataxia-telangiectasia-mutated (ATM) and NBS1-dependent phosphorylation of Chk1 on Ser-317 in response to ionizing radiation, J. Biol. Chem. 278 (2003) 14806–14811.
[49] C.S. Sørensen, R.G. Syljuåsen, J. Falck, T. Schroeder, L. Rönnstrand, K.K. Khanna, B.B. Zhou, J. Bartek, J. Lukas, Chk1 regulates the S phase checkpoint by coupling the physiological turnover and ionizing radiation-induced accelerated proteolysis of Cdc25A, Cancer Cell 3 (2003) 247–258.
[50] H.C. Reinhardt, M.B. Yaffe, Kinases that control the cell cycle in response to DNA damage: Chk1, Chk2, and MK2, Curr. Opin. Cell Biol. 21 (2009) 245–255.